Journal of Electroceramics, 14, 133–137, 2005

(Gd, Co, Ta)-Doped SnO_2 Varistor Ceramics

JIN-FENG WANG,* HONG-CUN CHEN, WEN-BIN SU, GUO-ZHONG ZANG, CHENG-JU ZHANG,
CHUN-MING WANG & PENG QI
School of Physics and Microelectronics, State Key laboratory of Crystal Materials, Shandong University, Ji'nan 250100, People's Republic of China

Submitted March 16, 2004; Revised August 25, 2004; Accepted August 27, 2004

Abstract. The effect on the microstructure and electrical properties of (Co, Ta)-doped SnO_2 varistors upon the addition of Gd_2O_3 was investigated. The threshold electric field of the SnO_2 based varistors increased significantly from 720 V/mm to 1455 V/mm, the relative dielectric constants of the SnO_2 based varistors decreased greatly from 833 to 330 as Gd_2O_3 concentration was increased up to 1.2 mol%. The significant decrease of the SnO_2 mean grain size, from 3.8 to 1.6 μm with increasing Gd_2O_3 concentration over the range of 0 to 1.2 mol%, is the origin for increase in the threshold voltage and decrease of the dielectric constants. The mean grain size reduction is attributed to the segregation of Gd_2O_3 at grain boundaries hindering the SnO_2 grains from conglomerating into large particles. Varistors were found to have superhigh threshold voltage and comparatively large nonlinear coefficient α. For 0.8 mol% Gd_2O_3-doped sample, threshold electrical field E and nonlinear coefficient α were measured to be 1125 V/mm and 24.0, for 1.2 mol% Gd_2O_3-doped sample, E and α were 1355 V/mm and 23.0. Superhigh threshold voltage and large nonlinear coefficient qualify the Gd-doped SnO_2 varistor as an excellent candidate in use for high voltage protection system.

Keywords: SnO_2, varistor, electrical nonlinearity, grain boundary barrier

Introduction

Varistor materials with high nonlinearity in their current-voltage characteristics are used as protecting devices against voltage transients in electronic and industrial equipment and as surge arrestors. The combination of high nonlinearity and high-energy absorption capability coupled with low power loss has made the ZnO varistor extremely attractive for high power applications [1–4]. However, with the increasing use of this device as the surge-suppressing element, the requirement of long-range-stability varistor is becoming more important.

In recent years, some papers have been published on novel SnO_2-based varistors. Pianaro et al. succeeded in preparing SnO_2-based varistor ceramics by doping with Co_2O_3 and Nb_2O_5, they found that SnO_2-based ceramics doped with 1.00 mol% CoO and 0.05 mol% Nb_2O_5 were a promising varistor material [5–9]. Wang et al. found that (Zn, Nb) doped SnO_2 and (Co, Sb) doped SnO_2 also exhibit varistor nonlinearity [10, 11].

In this paper, the effect of Gd_2O_3 addition on the properties of (Co, Ta)-doped SnO_2 varistors was investigated. It was found that Gd_2O_3 addition not only greatly raised the threshold voltage of the (Co, Ta)-doped SnO_2 varistors, but also significantly reduced the dielectric constant of the (Co, Ta)-doped SnO_2 varistors. The mean grain size reduction was attributed to the segregation of Gd_2O_3 at grain boundaries which hinder the SnO_2 grains from conglomerating into large particles.

Experimental Procedure

The composition used in mol% was: $(99.15 - x)\%$ $SnO_2 + 0.75\%\ Co_2O_3 + 0.1\%\ Ta_2O_5 + x\%\ Gd_2O_3$, with x: 0.0, 0.4, 0.8 and 1.2. The reagents used in

---

*Author to whom correspondence should be addressed. E-mail: wangjf@sdu.edu.cn

Table 1. Characteristics of (Gd, Co, Ta)-doped SnO_2 varistors.

Gd_2O_3 (mol%)	Mean grain size (μm)	α	Density (g/cm^3)	Relative density (%)	E_{1mA} (V/mm)	ϕ_B (eV)	ε_r (1 kHz)	R_{gb} ($\Omega \cdot$cm)	R_{gr} ($\Omega \cdot$cm)
0.00	3.8	14	6.80	97.8	610	1.14	833	52.9×10^6	1.50×10^3
0.4	2.6	23	6.78	97.5	935	1.13	545	24.5×10^6	1.95×10^3
0.8	2.0	24	6.76	97.2	1125	1.07	406	–	–
1.2	1.6	23	6.71	96.5	1355	1.02	330	21.2×10^6	2.35×10^3

Theoretical density of SnO_2 is 6.95 g/cm^3.

this study were analytical-grade SnO_2 (99.5%), Co_2O_3 (99.5%), Ta_2O_5 (99.95%) and Gd_2O_3 (99.95%). The chemicals were wet-milled in polyethylene bottles with ZrO_2 balls for 12 h in deionized water. The milled powders were dried, ground and granulated with PVA binder. The granulated powder were pressed into discs 15 mm in diameter by 1.0 mm in thickness at a pressure of 150 MPa. After burning out the PVA at 650°C, the discs were put into Al_2O_3 crucibles and fully surrounded with the powder of matching compositions, sintered in air at 1300°C for 1 hour and then cooled to room temperature freely. Silver paste was applied on the faces of the sintered discs to form electrodes by firing at 550°C. The sample phase was observed by X-ray diffraction (XRD) using CuKα radiation. For microstructure characterization, the samples were analyzed by scanning electron microscopy (SEM). For electrical characterization of current density versus applied electrical field, an I-V plotter (QT2) was used. The permittivity and the impedance were determined with impedance analyzer (Agilent 4294A) in the frequency range of 40 Hz–15 MHz. The electrical nonlinear coefficient α was obtained by

$$\alpha = \frac{\log(I_2/I_1)}{\log(V_2/V_1)}, \tag{1}$$

where V_1 and V_2 are, respectively, the voltage at current I_1 and I_2. For a Schottky type of mechanism, the current density of a varistor is related to the electric field and temperature by the equation [6]

$$J = AT^2 \exp[(\beta E^{1/2} - \phi_B)/kT], \tag{2}$$

where A is Richardson's constant, k is Boltzmann constant, ϕ_B is the interface barrier height, and β is a constant related to the grain size and the barrier width. In order to reduce the rise in temperature of the specimen caused by the electric current, we made the current flowing through the specimen in μA range and put the specimen in silicon oil. By use of equations

$$J_1 = AT^2 \exp\left[\left(\beta E_1^{1/2} - \phi_B\right)/kT\right], \tag{3}$$

$$J_2 = AT^2 \exp\left[\left(\beta E_2^{1/2} - \phi_B\right)/kT\right], \tag{4}$$

one can calculate ϕ_B. The data of the varistor system are listed in Table 1.

Results and Discussion

Figure 1 shows the X-ray diffraction pattern, (a) for the pure SnO_2 powder and (b) for SnO_2 varistor doped with 1.2 mol% Gd_2O_3. It was observed from the X-ray diffraction pattern that there was no apparent second any phases besides SnO_2 phase. Second any phases produced by dopants were too sparse to be detected by normal X-ray diffraction. The SEM micrographs of the as-fired surfaces of the varistors are shown in Fig. 2. It can be seen that the mean grain size of the SnO_2 based varistors decreases significantly, from 3.8 to 1.6 μm, with increasing Gd_2O_3 concentration. All varistors have densities as high as 96.5% or more of that of SnO_2 crystal. The electrical nonlinear characteristic of the varistor system is shown in Fig. 3. It was observed that the threshold voltage of the SnO_2-based varistors increased significantly from 720 V/mm to 1455 V/mm with increasing Gd_2O_3 concentration over the range of 0 to 1.2 mol%.

The thermogravimetric analysis suggests that the dopants of Co_2O_3 will be reduced to CoO with liberation of oxygen by the reaction [12]

$$Co_2O_3 \xrightarrow{950^\circ C} 2CoO + \frac{1}{2}O_2 \tag{5}$$

Considering that the ionic radius of Co^{2+} (0.078 nm) is close to that of Sn^{4+} (0.071 nm), the introduction of

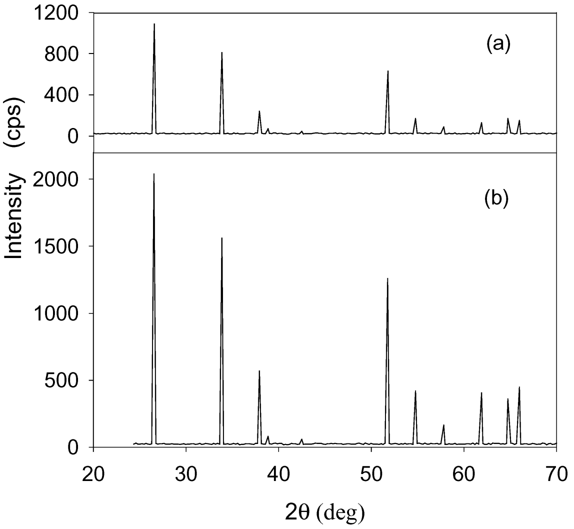

Fig. 1. X-ray diffraction, (a) pure SnO_2, (b) (Co, Ta)-doped SnO_2 varistor with 2.5 mol% Gd_2O_3.

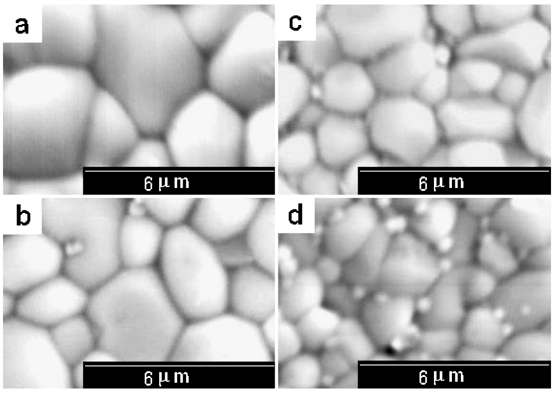

Fig. 2. SEM microstructure for $(99.15 - x)\%SnO_2 + 0.75\%Co_2O_3 + 0.1\%Ta_2O_5 + x\%\ Gd_2O_3$ varistors (a) $x = 0.0$, (b) $x = 1.5$, (c) $x = 2.0$, (d) $x = 2.5$.

CoO to the SnO_2 lattice should lead to the reaction

$$CoO \xrightarrow{SnO_2} Co''_{Sn} + V_O^{\bullet\bullet} + O_O^{\times} \qquad (6)$$

where the Kröger-Vink marks [13] were used. Due to a small difference between the ionic radius of Ta^{5+} (0.073 nm) and that of Sn^{4+}, the substitution of Sn^{4+} by Ta^{5+} is the most likely to occur. The reaction can be written as

$$Ta_2O_5 \xrightarrow{SnO_2} 2Ta^{\bullet}_{Sn} + 2e' + 4O_O^{\times} + \frac{1}{2}O_2 \qquad (7)$$

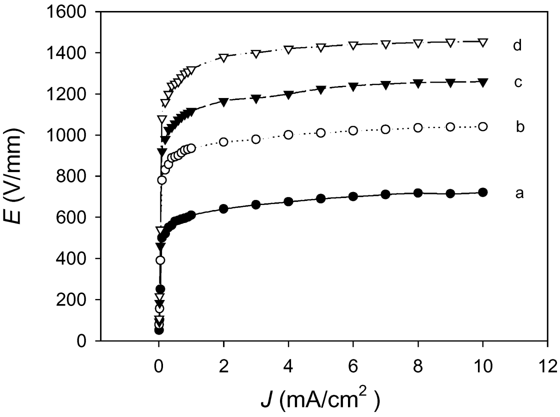

Fig. 3. Electric field versus current for $(99.15 - x)\%SnO_2 + 0.75\%Co_2O_3 + 0.1\%Ta_2O_5 + x\%\ Gd_2O_3$ varistors, (a) $x = 0.0$, (b) $x = 1.5$, (c) $x = 2.0$, (d) $x = 2.5$.

Oxygen in the above equations will be partly absorbed at SnO_2 grain boundaries

$$O_2 \rightarrow 2O^{\times}_{ad} \qquad (8)$$

Those absorbed oxygen easily capture electrons to become negatively charged ions

$$O^{\times}_{ad} + e' \rightarrow O'_{ad} \qquad (9)$$

$$O^{\times}_{ad} + 2e' \rightarrow O''_{ad} \qquad (10)$$

The role of the absorbed oxygen in the formation of boundary barriers was addressed in the literature [9, 14–16].

Because the ionic radius of Gd^{3+} (0.094 nm) are larger than that of Sn^{4+} (0.071 nm), the substitution of Sn^{4+} by Gd^{3+}, according to the reaction

$$Gd_2O_3 \xrightarrow{SnO_2} 2Gd'_{Sn} + V_O^{\bullet\bullet} + 3O_O^{\times} \qquad (11)$$

will cause SnO_2 lattice to distort. That is, the reaction of Eq. (11) is less likely to proceed than the reactions of Eqs. (6) and (7) because the the reaction of Eq. (11) causing lattice distortion should be more energetic than the reactions of Eqs. (6) and (7). Due to the partial substitution of Sn^{4+} by Gd^{3+}, much more Gd_2O_3 will have to reside at SnO_2 grain boundaries. Gd_2O_3 residing at SnO_2 grain boundaries may hinders the SnO_2 grains, on both sides of the boundary, from conglomerating into large particles. That may be the reason why the mean grain size of the SnO_2 based varistors decreased significantly with increasing Gd_2O_3 concentration.

The threshold voltage, V_s, for a varistor is determined by the mean number of barriers $\bar{N}$ in series multiplied by v_b

$$V_s = \bar{N}.v_b \tag{12}$$

where v_b is the barrier voltage at the grain boundary. From Table 1 we can see that the barrier height is roughly the same for the (Co, Ta, Gd)-doped SnO_2 varistors, therefore the threshold voltage, V_s, is roughly proportional to the mean number of barriers $\bar{N}$. If the thickness of a varistor is D and the mean grain size is d, it is clear from the relation $D = \bar{N}d$ that $\bar{N}$ is inversely proportional to mean grain size d. Thus, It is easily understood that the threshold voltage of the varistors increases significantly with increasing Gd_2O_3 concentration due to the significant reduction of the mean grain size with increasing Gd_2O_3 concentration.

The relative dielectric permittivity versus frequency for the varistor system is shown in Fig. 4. It is very clear that the dielectric constant of the varistor system decreases greatly with increasing Gd_2O_3 concentration. The relative dielectric constants can be expressed as the following relation [3]

$$\varepsilon_r = \varepsilon_B d/t_B \tag{13}$$

where ε_B is the internal permittivity of the barrier material, d is the mean grain size and t_B is the mean thickness of the insulation barrier. According to the Eq. (13), the permittivity of a varistor is proportional to the ratio d/t_B. From the fact in Table 1 that the barrier height is roughly the same for all Gd_2O_3-doped varistors one can deduce that the variation of t_B for all Gd_2O_3-doped varistors is small too. Therefore, the permittivity of the Gd_2O_3-doped varistors is mainly determined by the mean grain size d. So, the decrease of the permittivity of Gd_2O_3-doped varistors with increasing Gd_2O_3 concentration is reasonable because the SnO_2 mean grain size decreases significantly with increasing Gd_2O_3 concentration.

The impedance diagrams of $-Z''$ (negative reactance) vs Z' (resistance) of a varistor usually takes a form of a semicircle. But the impedance diagrams of $-Z''$ vs Z' of the Gd_2O_3-doped varistors measured at room temperature present a partial semicircle, which leads to a difficulty in distinguishing the contributions of boundaries from those of grains. To show a whole semicircle of the impedance diagrams of $-Z''$ vs Z' of the Gd_2O_3-doped varistors, high-temperature measurements at 250°C were performed. The impedance diagrams of $-Z''$ vs Z' of the Gd_2O_3-doped varistors are shown in Fig. 5. The resistivities of grains are determined to be approximately 1.50, 1.95, 2.35 $k\Omega \cdot cm$ at the frequency of 13 MHz for samples doped with 0.0, 0.4 and 1.2 mol% Gd_2O_3, the resistivities of grain boundaries are determined as 52.9, 24.5 and 21.2 $M\Omega \cdot cm$ at the frequency of 40 Hz, respectively. One can see that doping Gd_2O_3 causes the boundary resistivities to decrease and the grain resistivities to increase. Table 1 shows the characteristic detail of the varistor system.

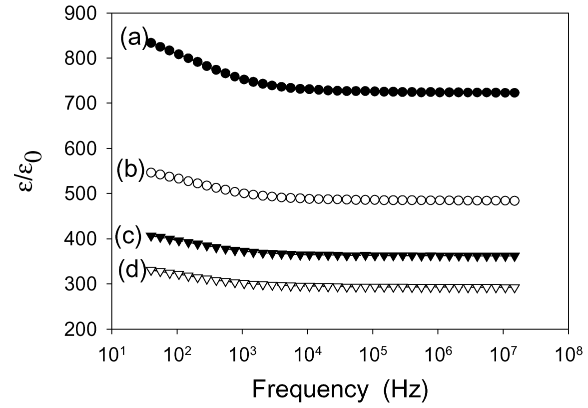

Fig. 4. Dielectric permmittivity versus frequency for $(99.15 - x)\%SnO_2 + 0.75\%Co_2O_3 + 0.1\%Ta_2O_5 + x\%\ Gd_2O_3$, (a) $x = 0.0$, (b) $x = 1.5$, (c) $x = 2.0$, (d) $x = 2.5$.

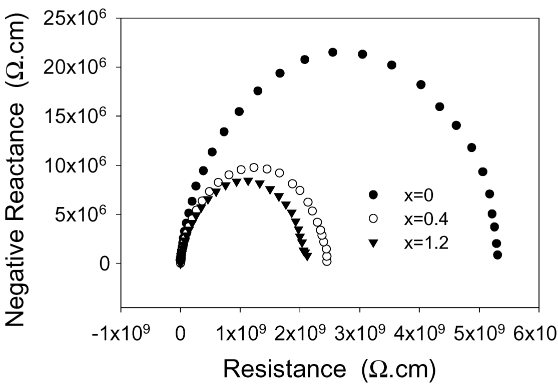

Fig. 5. Impedance diagrams for $(99.15 - x)\%SnO_2 + 0.75\%Co_2O_3 + 0.1\%Ta_2O_5 + x\%\ Gd_2O_3$.

Due to the lattice distortion caused by the substitution of Sn^{4+} with Gd^{3+}, the oxygen vacancy $V_O^{\cdot\cdot}$ in Eq. (11) is energetically unfavorable and may easier react with gaseous oxygen according to the equation

$$V_O^{\cdot\cdot} + \frac{1}{2}O_2 \rightarrow O_O^x + 2\text{holes}^{\cdot} \quad (14)$$

The recombination between the holes of Eq. (14) and the electrons in SnO_2 grains will result in the decrease in electrons concentration of SnO_2 grains. That may be the reason why the grain resistivity of the SnO_2-based varistors increased with increasing Gd_2O_3 concentration.

Conclusions

(1) Gd_2O_3 addition has a great effect on electrical properties of the (Co, Nb)-doped SnO_2. Gd_2O_3 can substantially raise the threshold voltage (Co, Ta)-doped SnO_2 and lower the permittivity of the (Co, Ta)-doped SnO_2. The significant decrease of the SnO_2 grain size, from 3.8 to 1.6 μm with increasing Gd_2O_3 concentration over the range of 0 to 1.2 mol%, is the origin for raising the threshold voltage and lowering the dielectric constants.

(2) Because the ionic radius of Gd^{3+} is larger than that of Sn^{4+}, the process of the substitution of Sn^{4+} by Gd^{3+} is relatively difficult to occur. Gd_2O_3 residing at SnO_2 grain boundaries may hinders the SnO_2 grains on its both sides from conglomerating into large particles. That may be the reason why the mean grain size of the SnO_2 based varistors decreased significantly with increasing Gd_2O_3 concentration.

(3) The SnO_2 varistors doped with 0.8 and 1.2 mol% Gd_2O_3 have superhigh threshold voltage and larger nonlinear coefficient α. Superhigh threshold voltage and quite larger nonlinear coefficient α qualify the Gd-doped SnO_2 varistor as an excellent candidate in use for the high voltage protection system.

Acknowlegment

This work was supported by the Natural Science Foundation of Shandong, China under Grant No. Z2003F04.

References

1. M. Matsuoka, *Jpn. J. Appl. Phys.*, **10**, 736 (1971).
2. T. Asokan and R. Freer, *J. Mater. Sci.*, **25**, 2447 (1990).
3. P.R. Emtage, *J. Appl. Phys.*, **48**, 4372 (1977).
4. T.K. Gupta, *J. Am. Ceram. Soc.*, **73**, 1817 (1990).
5. S.A. Pianaro, P.R. Bueno, E. Longo, and J.A. Varela, *J. Mater. Sci. Lett.*, **14**, 692 (1995).
6. S.A. Pianaro, P.R. Bueno, E. Longo, and J.A. Varela, *J. Mater. Sci. Lett.*, **16**, 634 (1997).
7. P.R. Bueno, S.A. Pianaro, E.C. Pereila, L.O.S. Bulhoes, et al., *J. Appl. Phys.*, **84**, 3700 (1998).
8. A.C. Antunes, S.R.M. Antunes, S.A. Pianaro, M.R. Rocha, et al., *J. Mater. Sci. Lett.*, **17**, 577 (1998).
9. E.R. Leite, A.M. Nascimento, P.R. Bueno, E. Longo, et al., *J. Mater. Sci. Mater. Electr.*, **10**, 321 (1999).
10. J.F. Wang, Y.J. Wang, W.B. Su, H.C. Chen, et al., *Mater. Sci. Eng. B*, **96**, 8 (2002).
11. C.P. Li, J.F. Wang, W.B. Su, H.C. Chen, et al., *Phsyica B*, **307**, 1 (2001).
12. J.A. Cerri, E.R. Leite, D. Guovea, E. Longo, and J.A. Varela, *J. Am. Ceram. Soc.*, **79**, 799 (1996).
13. F.A. Kröger, *The Chemistry of Imperfect Crystals* (Holland, Amsterdam, 1974).
14. M.R.C. Santos, P.R. Bueno, E. Longo, and J.A. Varela, *J. Eur. Ceram. Soc.*, **21**, 161 (2001).
15. F. Stucki and F. Greuter, *Appl. Phys. Lett.*, **57**, 446 (1990).
16. P.R. Bueno, E.R. Leite, M.M. Oliveira, M.O. Orlandi, and E. Longo, *Appl. Phys. Lett.*, **79**, 48 (2001).